Published by AIT
the Italian Society of Remote Sensing

Optical Detectors for Integration into a Low Cost Radiometric Device for In-Water Applications: HyDROW Performance Test at Loskop Dam

Naven Chetty[1]*, Arshath Ramkilowan[1], Derek J. Griffith[1] and Meena D. Lysko[2]

[1]School of Chemistry and Physics, University of KwaZulu-Natal, Private Bag X01, Scottsville 3209 Pietermaritzburg, S. Africa
[2]Defence, Peace, Safety and Security, Council for Scientific and Industrial Research, Pretoria, S. Africa
*Corresponding author, e-mail address: ChettyN3@ukzn.ac.za

Abstract
South Africa's fresh water resources are under threat by Harmful Algal Blooms (HABs). A comprehensive and cost effective method for wide area detection and monitoring of HABs is therefore needed to manage and where possible circumvent the negative impact HABs may have on the country's aquatic ecosystems. Current commercial radiometers used for such applications are often too costly to purchase in numbers. This study focuses on the performance of a low cost, in-house developed prototype radiometer, Hyperspectral Device for Radiometric Observations in Water (HyDROW). HyDROW's performance has been evaluated against data registered with a commercially available Hyperspectral Tethered Spectral Radiometer Buoy (HyperTSRB) during a field campaign at Loskop Dam in South Africa. The Loskop Dam is at risk for HABs and has been selected given its diverse environments from an optical perspective. Measurements were made at five optically diverse test points. The maximum percentage difference between the HyperTSRB and HyDROW were ~8% in the blue, ~19% in the green and ~24% in the red bands of the spectrum. The correlation coefficients between the radiometers range from 0.97 at the most turbid of test sites, to better than 0.99 in clearer waters.
Keywords: Optical detectors, radiometers, performance testing, low-cost radiometers, HyDROW.

Introduction

Eutrophication linked Harmful Algal Blooms (HABs) are severely threatening the health of underprivileged rural communities through exposure to polluted waters. Livestock and marine mortalities in addition to quality non-compliance in agriculture and aquaculture sectors resulting from these unsafe waters has led to the loss of revenue, directly impacting on the country's economy, as discussed by Bernard [2010]. Logistical and financial constraints prevent the

systematic and frequent monitoring of local water ecosystems required to lessen or altogether mitigate the adverse impact of HABs.

A novel research initiative, Safe Waters Earth Observation Systems (SWEOS), aims to improve on current water monitoring schemes in South Africa by coupling satellite-based remote sensing procedures with low-cost autonomous in-situ radiometric sensor systems. Such a system offers cost effective, frequent, and sustained observations using scalable techniques and technologies, with the ultimate aim of providing a comprehensive and cost effective system for wide area detection and monitoring of HABs in South Africa. Further information on SWEOS is provided by Bernard [2010] and Lysko et al. [2011].

Kohler and Philpot [2000] highlight the significance of the link between remotely sensed data and in situ data in the development and application of hyperspectral algorithms used to derive various optical properties of water bodies. Due to the dynamic nature of water bodies, linking in situ data from a single sensor location at a given time to the corresponding pixel in remotely sensed data may often prove insufficient. One possible solution to this is to increase the area being sampled for in situ measurements. Several successful attempts to capture water quality parameters in fresh water systems using sensors on board aircrafts have been reported (see for example, Hakvoort et al. [2002] and Koponen et al. [2002]).

While such a platform provides good spatial and spectral resolution and alleviates the aforementioned shortcoming of single stationed capturing of data, it is the temporal inconsistencies and the high costs associated with this method that make it less favourable to researchers in developing countries. The preferred solution, as hypothesized by the authors is to create a network of sensors, where each sensor is separated by a distance greater than the spatial resolution of the satellite sensor. The increase in size of the footprint of the in situ measurement will increase the confidence of the comparison to the remotely sensed imagery, additionally the accuracy and efficiency of the algorithms used to determine optical properties are improved.

Modern radiometers usually employed for in situ measurement taking are often too costly to purchase in large numbers and thus makes the forming of an in situ radiometer network impractical. One way to circumvent such a problem is to develop radiometers with a performance that is comparable to current commercially available instrumentation at a fraction of the cost. For this reason the development of Hyperspectral Device for Radiometric Observations in Water (HyDROW) is an invaluable facet of project SWEOS.

This study focuses on the performance evaluation of the prototype radiometer, HyDROW as an in-water upwelling radiance sensor. Data captured using the commercially available Hyperspectral Tethered Spectral Radiometer Buoy (HyperTSRB) during a field campaign on the Loskop Dam in South Africa is compared to analogous data captured using HyDROW. The results of this comparison provide as the performance indicator of HyDROW.

Description of the Hyperspectral Radiometers

The tethered buoy for the HyperTSRB provided a convenient platform for co-located observations with HyDROW during the Loskop Dam campaign. The coupling of the HyperTSRB and HyDROW gave both instruments the same viewing field which thereby reduced any scene bias.

HyperTSRB

The HyperTSRB system, from Satlantic, Inc., measures in-water upwelling radiance Lu ($\lambda_{400\text{ nm to }800\text{ nm}}$, z) at depth z = 0.66 m and downwelling irradiance Ed ($\lambda_{400\text{ nm to }800\text{ nm}}$, 0+ m)

just above the water surface. Each radiometer has a 256 channel silicon photodiode array with pixel size 25 μm x 2500 μm. The spectrograph has a 70 μm x 2500 μm entrance slit and a 10 nm spectral resolution. The full field of view in air and water are 8° and 3°, respectively. HyperTSRB compensates for thermal dark current changes that occur within the spectrograph with the use of a mechanical dark shutter that closes periodically in the radiometer. The HyperTSRB is configured with Satlantic's SatView application. SatView also logs the raw analogue to digital counts for subsequent conversion and post-processing. This work has used the Satlantic ProSoft 7.7.16 application for post-processing the raw counts to level 2 data. The level 2 data is calibrated and corrected with shutter dark readings and instrument immersion mode. The TSRB is advertised by Satlantic Inc. as having a compact design with low stray-light. It also has a 3.3 nm spectral resolution with less than 0.5 nm accuracy. This has resulted in the widespread implementation of the TSRB as a reference detector for airborne and spaceborne measurements, such as in work completed by [Cullen et al., 1997; Kohler and Philpot, 2000; Raqueno et al., 2005; Dwivedi et al., 2008]. The TSRB has been used for validation of or as input into radiative transfer models [Chang et al., 2003; Louchard et al., 2003]. Chang et al. [2003] also employ the use of the TSRB for radiometric comparisons between itself and the Ocena Colour Profiler (OCP-100). The prominent use of the TSRB in field experiments gives justification to it been used as a reference detector in this study.

HyDROW

HyDROW is a prototype developed by the Council for Scientific and Industrial Research (CSIR). Ramkilowan et al. [2013] have addressed the choice of spectrometer core for the radiometer. An optimized performance together with cost efficiency and field ruggedness had to be considered when deciding on the system electronics and radiometer housing. In gist, HyDROW's core is a miniaturized spectrometer with a linear 256 pixel CMOS array. Each pixel size is 12.5 μm x 1000 μm. The spectrometer entrance slit is 75 μm x 750 μm. The spectral response range is 340 nm to 750 nm and the spectral resolution is 10 nm. Together with fore-optic coupling, HyDROW has an 8° full field of view in air.

The absence of a shutter in the prototype technology leads to the obvious problem of not being able to separate background signal from the true signal. A temperature dependent calibration of the instrument allows for the dark signal to be characterised as a function of temperature, allowing for dark signal to be subtracted manually post-capturing of data. Mass production and in-house developing of host electronics is estimated at reducing the cost even further without compromising performance. The key features of HyDROW are summarised in Table 1.

HyDROW Calibration

HyDROW has been designed for in-water applications, which may include mooring at a permanent or semi-permanent site. For such cases prolonged exposure to sunlight, rough tides, natural contaminants and vandalism may threaten the reliability and consistency of the instrument data. It is therefore necessary for the radiometer to be frequently calibrated. The conventional and in-lab approach for calibration of radiometers employs the use of a calibrated reference radiometer together with a uniform and well defined light source having good spectral balance to characterise the response of the instrument. Such a calibration technique on a regular basis is often not feasible. Instead an in-field calibration

procedure should be implemented. Conventional field calibration lamps have a finite lifespan and cost in the region of $20000 [Slusser et al., 2000]. As the demand for in situ optical instrumentation increases, emphasis on the low cost increases too. The operational costs associated with calibration techniques incorporating conventional calibration light sources do not prove feasible. Instead the authors propose the following novel calibration methodology using a clear blue sky as a calibration source.

Table 1 - Instrument key feature description.

Parameter	Value	Unit
Price	8000	USD
Weight (in air)	1.402	kg
Dimensions (L x W)	280 x 100	mm
Detector	256 pixel CMOS array	-
FFOV (in air)	8	°
Spectral Resolution	10	nm
Spectral Sampling*1	1.73	nm
Wavelength Accuracy*2	±0.5	nm
SNR*3	10^4	-
Noise Equivalent Signal*3	10^2	-
Dynamic Range	10000:1	-

*1: wavelength determined by pixel fit to a 5th order polynomial. Sampling ranges from 1.46 at low pixel numbers to 1.88 nm at large pixel numbers. Mean value quoted in Table.

*2: measured under constant input conditions.

*3: using equations defined by Schaepman and Dangel [2000].

It is preferable that this calibration take place on a cloudless day, in the morning when aerosol concentrations are relatively low and less variable. The blue sky which is as a result of Rayleigh scattering offers sufficient spectral range for calibration of an instrument in the visible portion of the electromagnetic spectrum. In this procedure, a calibrated reference radiometer (eg. Fieldspec Analytical Spectral Device) and the test radiometer (in this case HyDROW) are mounted on a tripod and tilted at an equal angle of inclination so as to view the same patch of sky. This angle and the azimuthal orientation of the radiometers should be chosen so as to exclude direct view of the sun, glint, and any other background feature that will inhibit the true radiance signature of the sky. The sky radiance should then be captured at a series of exposure times.

The responsivity($R(\lambda)$)of the UUT is then calculated using equation 1, where $DN_{cal}(\lambda)$ is the wavelength dependent digital number captured during calibration with the UUT and $L_{ref}(\lambda)$ is the corresponding radiance captured with the reference radiometer. To achieve calibrated upwelling radiances from the UUT ($L_{uUUT}(\lambda)$), the dark corrected DN captured during in-water measurement bursts, ($DN(\lambda)$), are transformed according to equation 2. $I_f(\lambda)$ is the immersion factor (discussed later) and $C_f(\lambda)$ is a correction factor taking into account effects of stray-light, self-shading and other uncertainty contributors. In this research $C_f(\lambda)$ is taken as unity.

$$R(\lambda) = \frac{DN_{cal}(\lambda)}{L_{ref}(\lambda)} \quad [1]$$

$$L_{uUUT}(\lambda) = \frac{DN(\lambda)}{R(\lambda)} I_f(\lambda) C_f(\lambda) \quad [2]$$

Necessary statistical measures should be taken to ensure validity of calibration. This will be achieved in part by quantifying the spectral deviation of the sky radiance (using the reference radiometer). This value should then be incorporated into the traceability of the final radiance values calculated. In the period leading up to the field calibration, the relevant aerosol optical parameters should be monitored for consistency. This would allow for calibration to take place at the most optimum time.

Advantages

This field calibration technique offers a free and reliable alternative to the conventional lab or field calibration procedures. An obvious advantage of this method of calibration is that it allows for on-site calibration provided weather conditions are suitable and that the aerosol and molecular content are monitored.

Limitations

It should be noted that the success of this methodology depends heavily on the local environmental conditions; Loskop during late-winter exhibited stable atmospheric conditions which justified the use of this field calibration technique. The conventional methods as described in Schaepman and Dangel [2000] and Slusser et al. [2000] will be reverted to when temporal variability in local conditions are less than the time required to make the necessary calibration measurements. To negate the effects of any spatial non-uniformity that may be present in the sky radiance it is advisable to choose a reference radiometer with an acceptance field-of-view equivalent to the unit under test, baffling should be introduced when the matching of FOV's is not possible.

Sample Sites

Sample sites on the Loskop Dam were determined primarily with two criteria: a) representation of various regions, and b) representation of various optical water types in the lake.

Loskop Dam is located in Mpumalanga province about 100 km northeast of the city, Pretoria (25.43°S, 29.34°E). It is a single water body with pronounced changes in turbidity levels along its length as evident from Oberholster et al. [2009] and Oberholster et al. [2012]. Optically turbid zones have been found near the river inlet, with progressively clearer waters closer to the main basin. This optical turbidity range within a single water body is uncommon and has provided the basis to probe HyDROW's quality, accuracy and reliability across a dynamic turbidity range.

Five sample sites were selected along the length of the dam as shown in Figure 1. The environment condition per site is given in the Table 2. The range of Secchi disk depths (Tab. 1), measured during the field trial, is an indication of variation in optical turbidity.

Table 2 - Environment conditions at sample sites on 8 August 2011.

	River Inlet	Ceratium	Buoy	Lacustrine	Main Basin
Location	25.495°S, 29.245°E	25.488°S, 29.264°E	25.465°S, 29.259°E	25.468°S, 29.279°E	25.430°S, 29.323°E
Site arrival time GMT+2	09H00	09H40	10H30	11H00	11H30
Wind	3.0 mph NW	5.5 mph SW	4.5 mph SW	2.5 mph NE	None
Wave height	~ 1 cm	~ 2 cm	~ 2 cm	~ 2 cm	~ 1 cm
Cloud cover	~ 75 %	< 10 %	< 10 %	< 10 %	< 10 %
Mean Secchi disk depth	193 cm	45 cm	325 cm	438 cm	654 cm

Data Capturing Methodology

The Loskop Dam field data for this comparison was collected on 8 August 2011. The HyperTSRB's tethered mooring provided the ideal platform as HyDROW could be secured side by side with the upwelling radiance sensor of the HyperTSRB. Special effort was put into ensuring that neither radiometer had a compromised field of view. The norm, as shown in Mueller [2003] and Barker [2011] is to allow the buoy to sit at the water surface a distance of at least 30 m from the boat. The buoy was hand-deployed during the campaign and was therefore within 1 m from the boat. A concerted effort was made to ensure that no bubbles collected at the water-lens interface and that shadowing from the boat and the moored system itself was negated as far as possible.

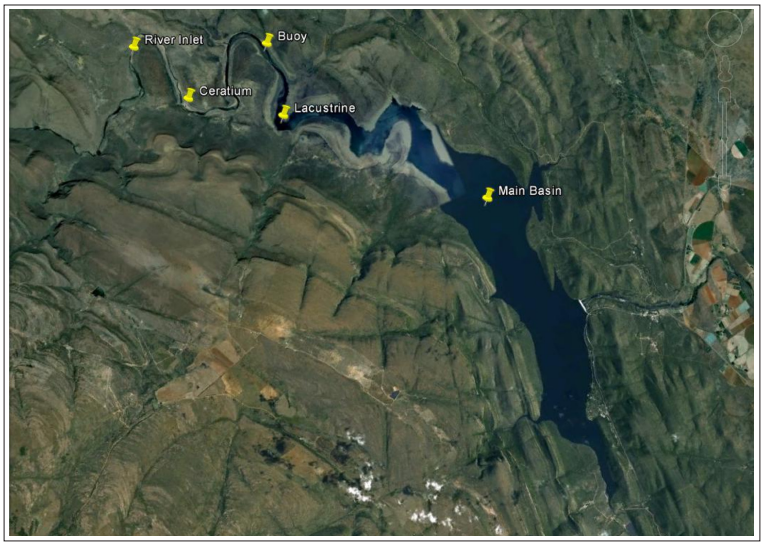

Figure 1 - Google Earth image over Loskop Dam with the five sample sites.

To be able to interpret the data captured from the HyDROW, HyperTSRB reference radiometric data was captured simultaneously. Data sets were acquired in 3 minute bursts with exposure times ranging from 250 to 1000 ms. The user defined exposure time for HyDROW was chosen so as to be within 1 ms of the optimised exposure time set by

HyperTSRB. Between 100 and 200 samples per wavelength were averaged to account for the waters inherent optical variability. Secchi disk readings were taken at each sample site and allowed for a relationship to be formed between the performance of HyDROW and the clarity of a given water sample.

Data Comparison

The Lu (λ, 0.66 m) spectra from both HyperTSRB and HyDROW are relatively constant in shape (see Fig. 2) for four of the sample sites: Buoy, Lacustrine, Main Basin and River Inlet. The data from Ceratium is plotted separately in Figure 3. A large relative standard deviation (RSD) for this site is expected given the significant optical turbidity with the higher concentration of large-celled dinoflagellate. The distinct step feature at about 590 nm and the sharp peak at 725 nm is followed by both the unit under test and the reference. The relative deviation plots from the second column in Figure 2. show that disagreement between HyperTSRB and HyDROW is below 10 % between 450 nm and 550 nm and within 30 % for wavelengths exceeding 550 nm.

The correlation between LuHyDROW (λ, 0.66 m) and LuHyperTSRB (λ, 0.66 m) for each sample site has been calculated using the Pearson's product moment correlation coefficient *r* [Bhattacharyya et al., 1977]. That is:

$$r = \frac{\sum_{i=1}^{n}(X_i - \overline{X})(Y_i - \overline{Y})}{\sqrt{\left[\sum_{i=1}^{n}(X_i - \overline{X})^2\right]\left[\sum_{i=1}^{n}(Y_i - \overline{Y})^2\right]}}, \quad [3]$$

where (X_1, Y_1), … (X_n, Y_n) are the n pairs of observations. It is seen from Table 3 that r is above 0.99 for all sample sites except for Ceratium ($r = 0.97$). As expected, *r* also increases as the water clarity increases.

Table 3 - Correlation between HyDROW and TSRB and relation to mean Secchi disk depth.

	Main Basin	Lacustrine	Buoy	River Inlet	Ceratium
Mean Secchi disk depth	654 cm	438	325 cm	193 cm	45 cm
Correlation coefficient, *r*	0.9946	0.9948	0.9921	0.9905	0.9744

Considered Error Factors

Accurate in-water radiometric measurements in an uncontrolled environment are a challenge. The instrument design, calibration, measurement protocol and errors associated with environmental effects contribute to large measurement uncertainties. As an example, [Hooker, 2000] reports an in-water up-welling radiance Lu (*z* = depth down to 1 % light level, 510 nm) deviation of up to 25 % between two radiance profilers that were deployed by winch. Much effort has therefore been made to identify and decrease uncertainties. It is noted that the advancement of optical instrumentation technology and studies such as Leathers et al. [2001], Torrecilla et al. [2008] and Ohde et al. [2003] address the most significant sources of radiometric uncertainty in measurements of Lu (z, λ) and suggest methods to investigate and reduce errors due to instrument self-shading, tilt, stray light, immersion and depth differences.

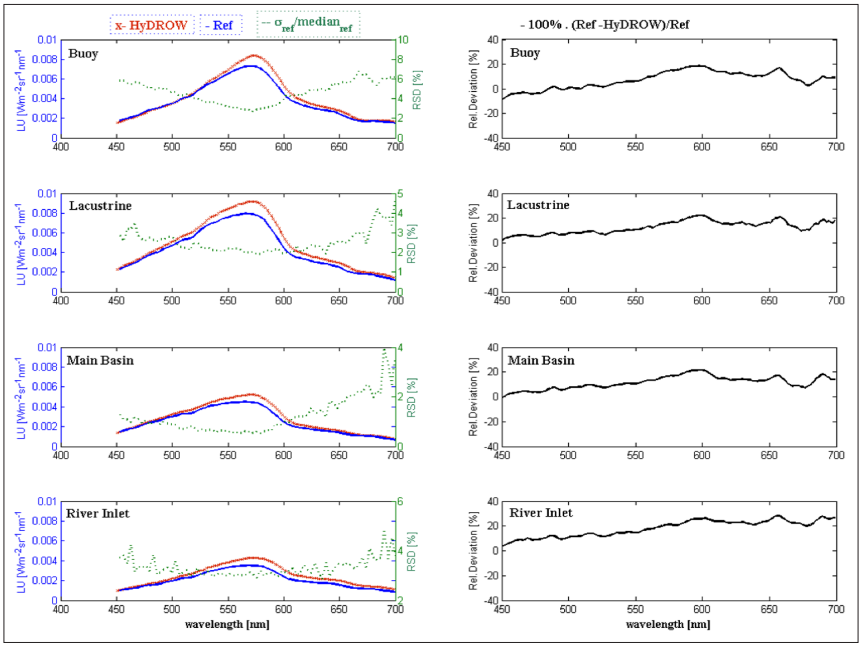

Figure 2 - Column1: Lu(λ, 0.66 m) from HyperTSRB and HyDROW per sample site, with the RSD from HyperTSRB. Column2: HyDROW Lu(λ, 0.66 m) deviation relative to HyperTSRB.

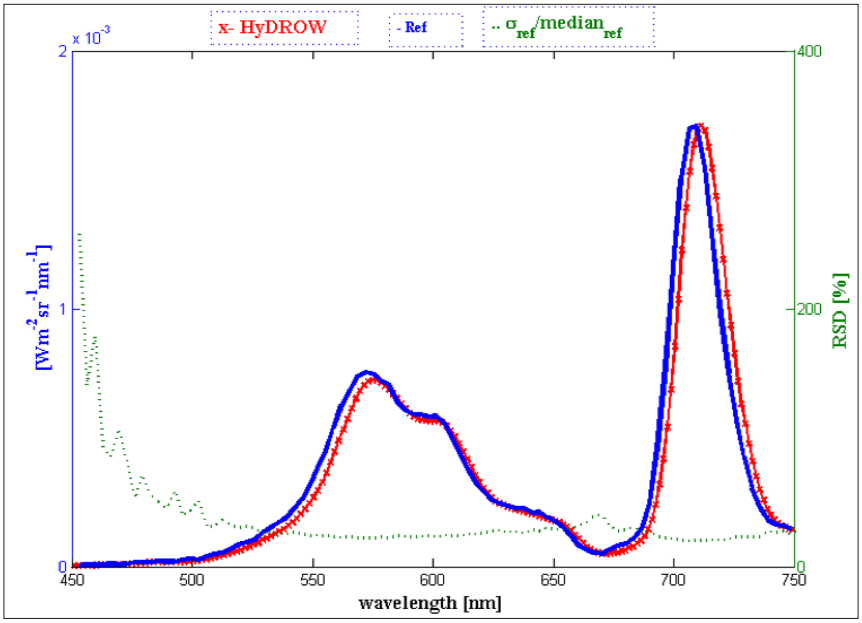

Figure 3 - Lu (λ, 0.66 m) from HyperTSRB and HyDROW at sample site Ceratium, with the RSD from HyperTSRB.

Immersion factors

When a light detecting device is used in a medium different to that in which it was calibrated, the change in refractive index of the intervening medium (in this case water) causes alterations in absolute spectral response. An immersion factor is used to compensate for the difference in response of the instrument. Two effects influence in-water radiance measurements. Firstly the refractive index at glass-air interface (during calibration) differs from the refractive index of the glass-water interface (during in-water measurements). Secondly when submerged in water the field of view solid angle of the instrument is reduced allowing a smaller percentage of the radiance to be detected. Ohde et al. [2003] references an equation for the wavelength dependent immersion factor.

$$I_f(\lambda) = \frac{n_w(\lambda)[n_w(\lambda) + n_g(\lambda)]^2}{(1 + n_g(\lambda))^2} \quad [4]$$

Here n_w is the refractive index of the water and n_g is the refractive index of the glass window of the instrument. The wavelength dependence of n_g can be calculated from the Sellmeier equation:

$$n_g^2(\lambda) = 1 + \frac{B_1\lambda^2}{\lambda^2 - C_1} + \frac{B_2\lambda^2}{\lambda^2 - C_2} + \frac{B_3\lambda^2}{\lambda^2 - C_3} \quad [5]$$

where the coefficients are the experimentally determined Sellmeier coefficients given in Table 4.

Table 4 - Constants of dispersion for equation [3] to determine HyDROW's If.

	Constants of dispersion [Schott, 2011]
B1	1.03961212
B2	0.231792344
B3	1.01046945
C1	0.00600069867
C2	0.0200179144
C3	103.560653

The freshwater system in which HyDROW was tested consisted of organic assemblages which made n_w a variable quantity. Given that the purpose of this research was to measure the instrument's relative and not absolute performance, the consistent value of $n_w = 1.345$ employed for fresh water by the reference radiometer was adopted. The fundamental changes in refractive index due to temperature fluctuations are noted and estimated to contribute less than 1% over the operational temperatures. While n_w is likely to differ from the true index of refraction of the water, the consistent use of it for both instruments reduces the relative error.

Self-shading

The contribution of self-shading to an immersed radiometer is dependent on the geometry of the radiometer and platform, the absorption coefficient of the medium, the Sun zenith and the atmospheric turbidity. It is noted that average self-shading errors for the upwelling radiance of the HyperTSRB is about 5 % [Leathers et al., 2001]. However, as a system, LuHyDROW (λ, 0.66 m) relative to LuHyperTSRB (λ, 0.66 m) is not expected to have a significant bias due to self-shading since both instruments are strapped under the same bouy such that the differential effect of shadowing due to the buoy would be minimal. In this study, self-shading for the individual instruments has not been corrected for.

Stray-light

The high spectral resolution of hyperspectral radiometers provides the advantage to discern a target's fine-scale spectral features. The spectral selection in systems such as HyperTSRB and HyDROW is accomplished with a fixed dispersive optical train. The upwelling radiance signature is captured as an image of the entrance slit onto the detector array. Ideally, the image should be consistent with the spectral components of the target, within the instrument's bandpass. In practice, the imaged signature may be modified due to radiation from out-of-band wavelengths which activates a signal at the detector element. The modification is seen as instrumental stray-light. The sources of instrumental stray-light include ambient light distribution, scattered light from imperfect optical components, reflections off non-optical components and overlap from multiple order diffraction. Stray-light may cause the measured upwelling radiance to be erroneously high.

As shown in [Satlantic Inc., 2008], stray-light contribution to LuHyperTSRB (λ, z) can be up to 2 orders of magnitude higher than the true signal in extreme cases. With stray-light correction, stray-light contribution can be reduced to less than 0.2% (for 450 nm to 800 nm) and less than 2 % (for 350 nm to 450 nm). It is noted that LuHyperTSRB (λ, 0.66 m) data from the Loskop Dam campaign is not stray-light corrected. This can be done after a re-calibration of the HyperTSRB and with data processed with ProSoft 8.0.

Instrument stray-light can be resolved by using sufficiently narrow spectral band sources with sufficient output power [Zong et al., 2006]. This approach is not always practical. A selection of spectral cut-on filters against a uniform broad-band light source has been used to gauge the stray-light performance of HyDROW. For each filter, the net signal below the cut-on wavelength is considered as stray-light. Net stray-light was found to be less than 5 % with each of the cut-on filters (see Tab. 5). The limited set of cut-on filters does not allow for a complete characterisation of HyDROW for stray-light. LuHyDROW (λ, 0.66 m) data from the Loskop Dam campaign is therefore not stray-light corrected.

Table 5 - HyDROW net stray-light for 3 cut-on filters.

Filter Cut-on Wavelength	Net Stray-Light
517 nm	0.5 %
622 nm	1.9 %
667 nm	4.2 %

Summary
The Loskop Dam, with its spatially diverse optical turbidity, has been a convenient environment to test the radiometric performance of the HyDROW in measuring in-water upwelling radiance.
Table 6 indicates the comparison of HyDROW to HyperTSRB at key wavelengths. Tabulated alongside are analogous values for the Satlantic Inc. Ocean Colour Profiler (OCP-100) and HyperTSRB made by Chang et al. [2003]. Also included are the respective r^2 values based on the average of all data collected.
An absolute comparison cannot be drawn from Table 5 because these comparisons took place on different days at different locations and in different water types. However, given that Loskop Dam included oligotrophic, mesotrophic, eutrophic and hypereutrophic test-sites, and the relative accuracy at each site showed little variation, HyDROW, a first iteration, low-cost (less than half the price of commercially available instruments) prototype radiometer shows a lot of promise. The maximum percentage difference between the HyperTSRB and HyDROW were ~8% in the blue, ~19% in the green and ~24% in the red bands of the spectrum. The correlation coefficients between the radiometers range from 0.97 at the most turbid of test sites, to better than 0.99 in clearer waters.
Further characterization of the uncertainty contributors and enhancements to the calibration procedures are expected to improve the accuracy of the next generation prototype.

Table 6 - Percentage difference and r^2 comparison between HyperTSRB and OCP and HyperTSRB and HyDROW during their respective field campaigns.

	Wavelength (nm)					
	490	**532**	**555**	**590**	**682**	r^2
Hyper TSRB vs OCP	17	11	10	18	11	0.93
Hyper TSRB vs HyDROW	8	9	10	20	10	0.99

Acknowledgements
Authors Ramkilowan and Griffith would like to thank the Defence, Peace, Safety and Security (DPSS) division at the Council for Scientific and Industrial Research (CSIR) in Pretoria which has provided the necessary expertise and funding to complete this project. Both Ramkilowan and Griffith were employed at DPSS for the duration of this study.

References
Barker K. (2011) - *MERIS Optical Measurement Protocols*. Part A: In-situ water reflectance measurements. CO-SCI-ARG-TN-008, http://hermes.acri.fr/mermaid/dataproto (last accessed 07/02/2012).
Bernard S. (2010) - *Research proposal on Safe Waters Earth Observation Systems (SWEOS)*, CSIR, (unpublished report).
Bhattacharyya G.K., Johnson R.A. (1977) - *Statistical concepts and methods*. John Wiley & Sons, USA.
Chang G.C., Dickey T.D., Mobley C.D., Boss E., Pegau W.S. (2003) - *Toward closure of upwelling radiance in coastal waters*. Applied Optics, 42 (9): 1574 - 1582. doi: http://dx.doi.org/10.1364/AO.42.001574.
Cullen J.J., Ciotti A.M., Davis R.F., Lewis M.R. (1997) - *Optical detection and assessment*

of algal blooms. Journal of Limnology and Oceanography, 42 (5): 1223-1239. doi: http://dx.doi.org/10.4319/lo.1997.42.5_part_2.1223.

Dwivedi M.R., Babu K.N., Singh S.K., Vyas N.K., Matondkar S.G.P. (2008) - *Formation of algal bloom in the northern Arabian Sea deep waters during January-March: a study using pooled in situ and satellite data.* International Journal of Remote Sensing, 29 (15): 4537-4551. doi: http://dx.doi.org/10.1080/01431160802029693.

Hakvoort H., De Haan J., Jordans R., Vos R., Peters S. Rijkeboer M. (2002) - *Towards airborne remote sensing of water quality in The Netherlands-validation and error analysis*. ISPRS Journal of Photogrammetry and Remote Sensing, 57 (3): 171-183. doi: http://dx.doi.org/10.1016/S0924-2716(02)00120-X.

Hooker S.B., Maritorena S. (2000) - *An Evaluation of Oceanographic Radiometers and Deployment Methodologies*. Journal of Atmospheric and Oceanic Technology, 17: 811-830. doi: http://dx.doi.org/10.1175/1520-0426(2000)017<0811:AEOORA>2.0.CO;2.

Kohler D.D.R., Philpot W.D. (2000) - *Comparing in situ and remotely sensed measurements in optically shallow waters*. Ocean Optics XV, pp. 16-20.

Koponen S., Pulliainen J., Kallio K., Hallikainen M. (2002) - *Lake water quality classification with airborne Hyperspectral spectrometer and simulated MERIS data*. Remote Sensing of Environment, 79 (1): 51-59. doi: http://dx.doi.org/10.1016/S0034-4257(01)00238-3.

Leathers R.A., Downes T.V., Mobley C.D. (2001) - *Self-shading correction for upwelling sea-surface radiance measurements made with buoyed instruments.* Optics Express, 8 (10): 561-570. doi: http://dx.doi.org/10.1364/OE.8.000561.

Louchard E.M., Reid R.P., Stephens F.C., Davis C.O., Leathers R.A., Downes T.V. (2003) - *Optical remote sensing of benthic habitats and bathymetry in coastal environments at Lee Stocking Island, Bahamas: A comparative spectral classification approach*. Journal of Limnology and Oceanography, 48 (1): 511-521. doi: http://dx.doi.org/10.4319/lo.2003.48.1_part_2.0511.

Lysko M.D., Griffith D.J., Ramkilowan A., Govender P. (2011) - *SWEOS annual report*. CSIR, 6700-SWEOS-59520-01 (unpublished report).

Mueller J.L., Fargion G.S., McClain C.R. (2003) - *Ocean Optics Protocols For Satellite Ocean Color Sensor Validation*. Revision 4, Volume VI: Special Topics in Ocean Optics Protocols and Appendices. NASA/TM-2003-211621/Rev4-Vol.VI.

Oberholster P.J., Myburgh J.G., Ashton P.J., Botha A.M. (2009) - *Responses of phytoplankton upon exposure to a mixture of acid mine drainage and high levels of nutrient pollution in Lake Loskop, South Africa.* Ecotoxicology and Environmental Safety, 73: 326-335. doi: http://dx.doi.org/10.1016/j.ecoenv.2009.08.011.

Oberholster P.J., Myburgh J.G., Ashton P.J., Coetzee J.J., Botha A.M. (2012) - *Bioaccumulation of aluminium and iron in the food chain of Lake Loskop, South Africa.* Ecotoxicology and Environmental Safety, 75: 134-141. doi: http://dx.doi.org/10.1016/j.ecoenv.2011.08.018.

Ohde T., Siegel H. (2003) - *Derivation of immersion factors for the hyperspectral TriOS radiance sensor*. Journal of Optics A: Pure and Applied Optics 5 (3): L12-L14. doi: http://dx.doi.org/10.1088/1464-4258/5/3/103.

Ramkilowan A., Chetty N., Griffith D.J., Lysko M.D. (2013) - *Optical Detectors for Integration into a Low Cost Radiometric Device for In-Water Applications: A Feasibility Study*. Indian Journal of Remote Sensing.

Raqueno R.V., Raqueno N.G., Weidemann A.D., Effler S.W., Perkins M., Vodacek A., Schott J.R., Philpot W.D., Kim M. (2005) - *Megacollect 2004: Hyperspectral Collection Experiment Over the Waters of the Rochester Embayment*. In *Algorithms and Technologies for Multispectral, Hyperspectral, and Ultraspectral Imagery XI*, edited by Sylvia S. Shen, Paul E. Lewis, Proceedings of SPIE, 5806: 566 - 577.

Satlantic Incorporated (2008) - ProSoft 8.0 User Manual. Document Number: SAT-DN-00228, Revision: 8.0B.

Schaepman M.E., Dangel S. (2000) - *Solid laboratory of calibration of a non-imaging spectroradiometer*. Applied Optics, 39 (21): 3754-3764. doi: http://dx.doi.org/10.1364/AO.39.003754.

Schott A.G. (2011) - *Optical glass data sheet.* Germany.

Slusser J., Gibson J., Bigelow D., Kolinski D., Disterhoft P., Lantz K., Beaubien A. (2000) - *Langley method of calibrating UV filter radiometers*. Journal of geophysical research, 105 (D4): 4841-4849. doi: http://dx.doi.org/10.1029/1999JD900451.

Torrecilla E., Pons S., Vilaseca M., Piera J., Pujol J. (2008) - *Stray-light correction of in-water array spectroradiometers.* Effects on underwater optical. IEEE OCEANS 2008, 1-7.

Zong Y., Brown S.W., Johnson B.C., Lykke K.R., Ohno Y. (2006) - A Simple *Stray-light Correction Method for Array Spectroradiometers*. Applied Optics, 45 (6): 1111-1119. doi: http://dx.doi.org/10.1364/AO.45.001111.

Received 04/07/2012, accepted 05/02/2013